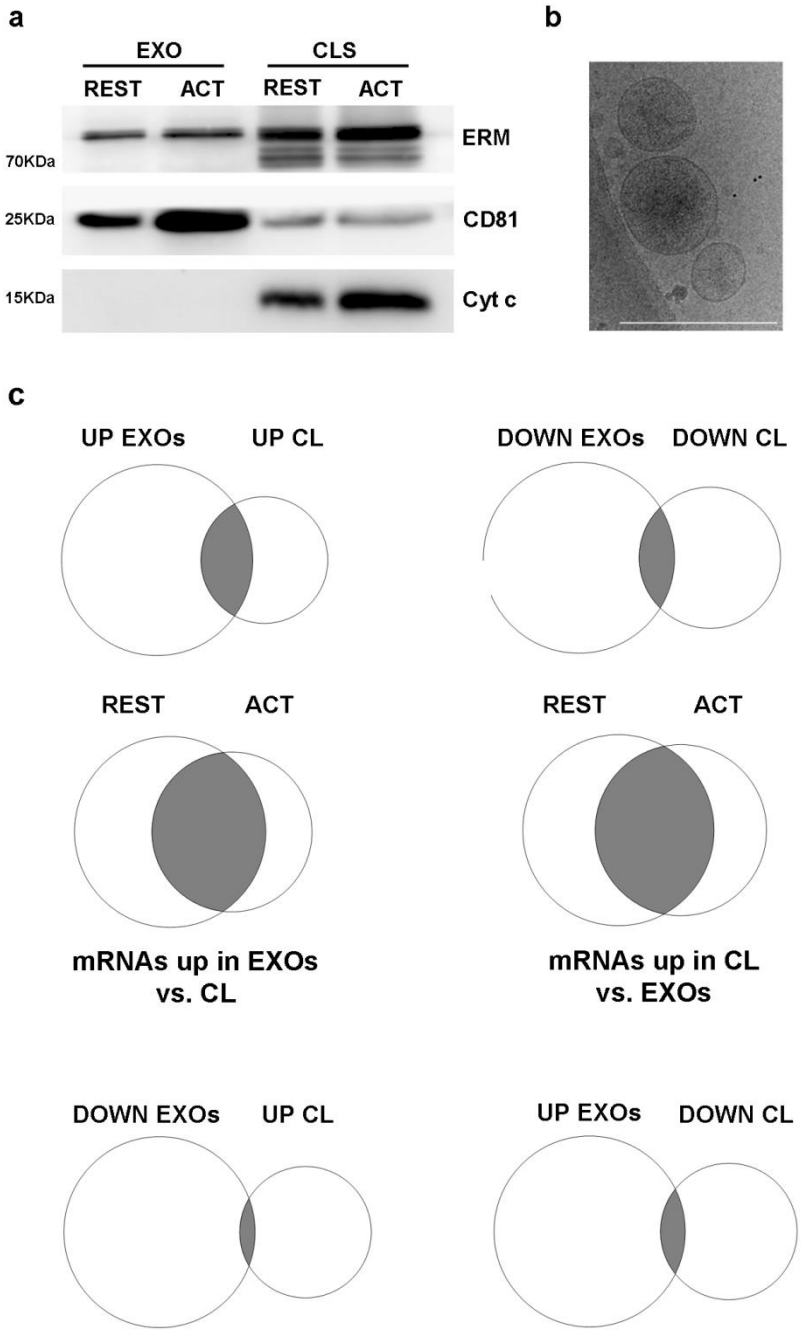

Supplementary Figure S1. Venn diagram analysis of mRNA microarray data and miRNA target analysis. (a) Western blot analysis of T lymphoblasts (CLS) and their exosomes (EXO) in resting (REST) and activated (ACT) conditions. Exosome sample purity was assessed by the presence of exosome markers (CD81, ERMs) and the absence of cytochrome c (cyt c). **(b)** Cryo-fracture transmission electron microscopy images of isolated exosomes. Scale bar 200 nm. **(c)** Upper panels: Activation-induced changes in mRNA profile differ between T cells and their derived exosomes. Middle panels: Some mRNAs are always specifically sorted into exosomes (left) or specifically retained in cells (right), independently of the activation state of the T cell. Lower panels: Some mRNAs are upregulated in cells upon activation but downregulated in exosomes (left) and *vice versa* (right).

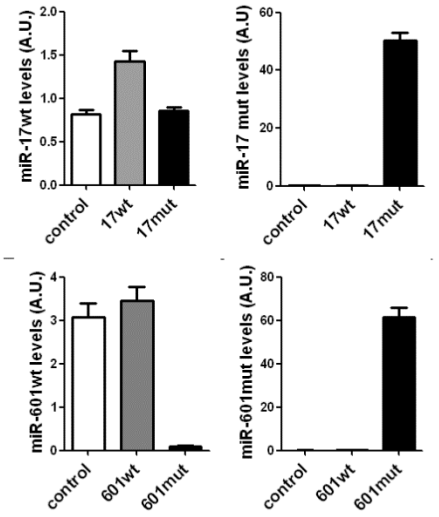

Supplementary Figure S2. LNA-specific primers allow discrimination between wild-type and mutated miRNAs. Upper panels: qPCR analysis of miR-17wt and miR-17mut levels in control cells, cells transfected with miR-17wt, and cells transfected with miR-17mut. miR-17wt is overexpressed in cells transfected with miR-17wt plasmid but not in cells transfected with miR-17mut plasmid, and miR-17mut is only detected in cells transfected with miR-17mut plasmid. Lower panels: qPCR analysis of miR-601wt and miR601mut levels in control cells, cells transfected with miR601wt, and cells transfected with miR-601mut. We could discriminate between miR-601wt and miR-601mut; however, cells transfected with miR-601wt plasmid barely overexpressed miR-601, and cells transfected with miR-601mut downregulated endogenous miR-601wt expression, indicating that stringent compensation mechanisms operate to maintain low miR-601 levels in cells. N=3. Error bars indicate s.d.

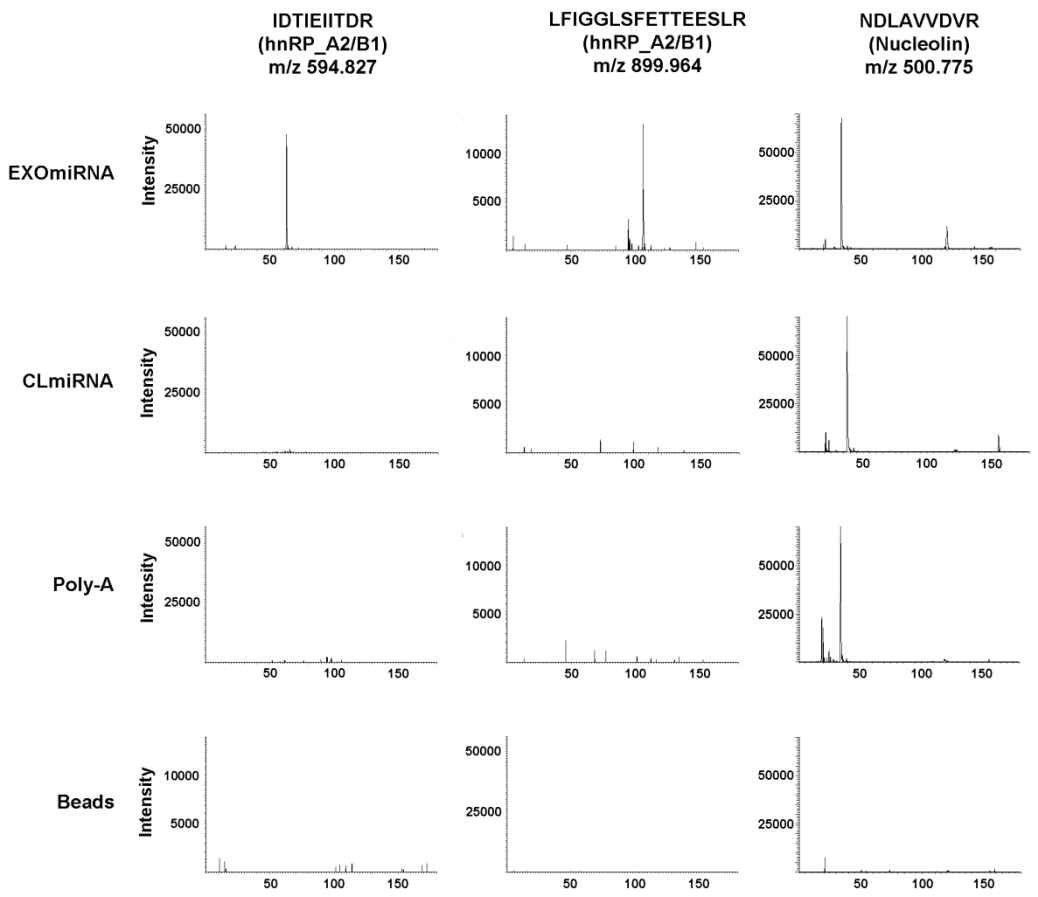

Supplementary Figure S3. Proteomic analysis of hnRNPA2B1 binding to EXOmiRNAs. Complete ion chromatogram traces of the monoisotopic peaks corresponding to the indicated peptides, identified from hnRNPA2B1 or from a non-specifically binding protein (nucleolin).

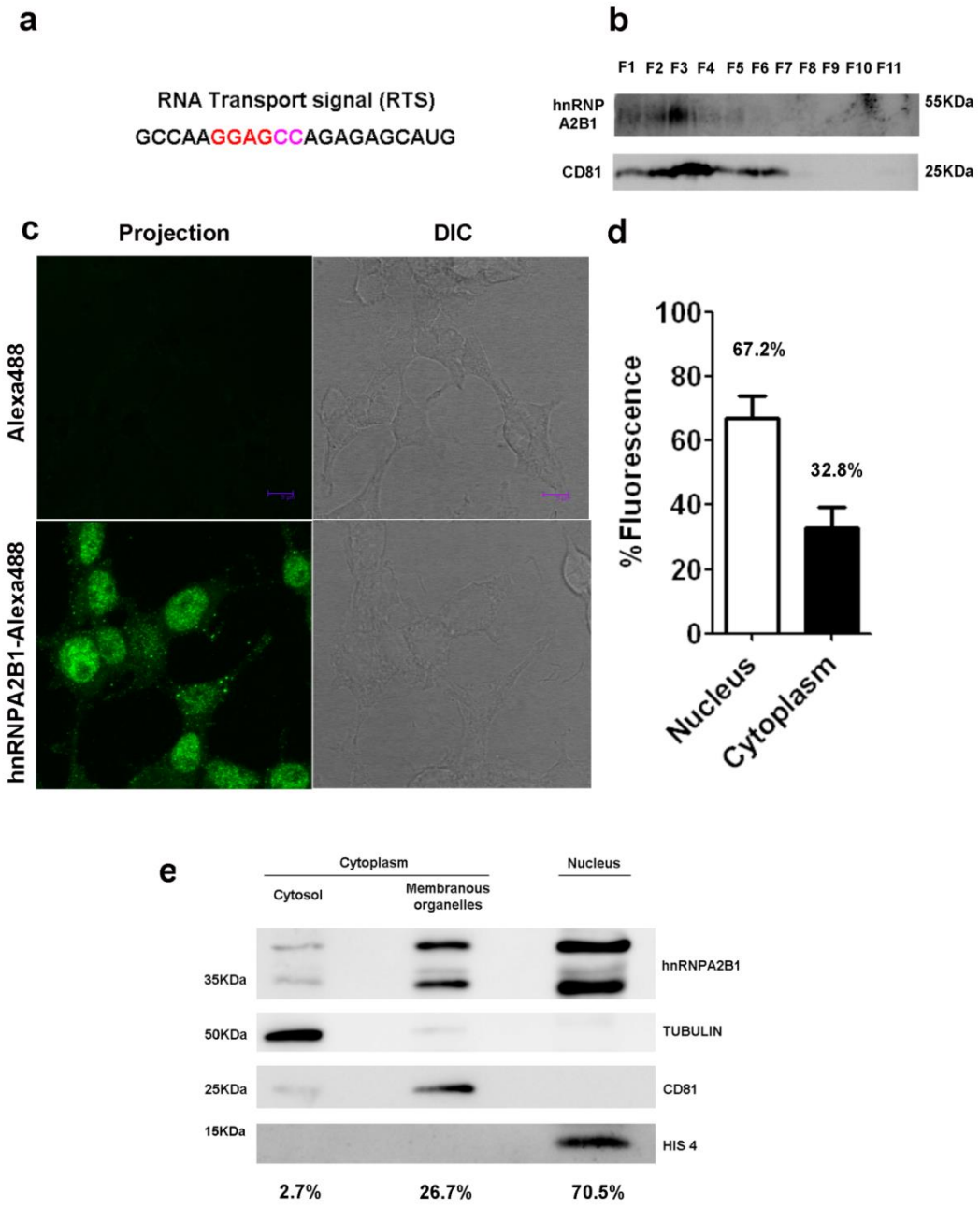

Supplementary Figure S4. HnRNPA2B1 presence in exosomes (a) RNA transport signal sequence (RTS) **(b)** Western blot showing hnRNPA2B1 and CD81 enrichment in sucrose fraction 3. Exosomes were overlaid with a linear sucrose gradient and floated into the gradient by centrifugation. Gradient fractions were collected and analyzed by western blot. **(c)** Confocal microscopy detection of hnRNPA2B1 (green) in nucleus and cytoplasmic granules of HEK293T cells. Cells were stained with hnRNPA2B1 and secondary antibodies (Alexa488) or only with secondary antibody as a negative control. Images show maximal projections of confocal images and the DIC images. Scale bar, 9 μm. **(d)** Quantification of hnRNPA2B1 localization in nucleus and cytoplasm by confocal analysis. Bars represent the percentage of hnRNPA2B1 fluorescence in nucleus and cytoplasm per cell. Numbers above represent the average percentage. Error

bars represent standard deviation. n= 105 cells coming from three independent experiments. **(e)** Western blot analysis of hnRNPA2B1 in subcellular fractions. Jurkat T cells subcellular compartments were fractionated. Cytosol, membranous organelles and nucleus fractions were blotted for hnRNPA2B1, tubulin (cytosol marker), CD81 (membrane marker) and Histone 4 (nucleus marker). Numbers represent the percentage of hnRNPA2B1 in each fraction with respect to total hnRNPA2B1 (sum of all fractions).

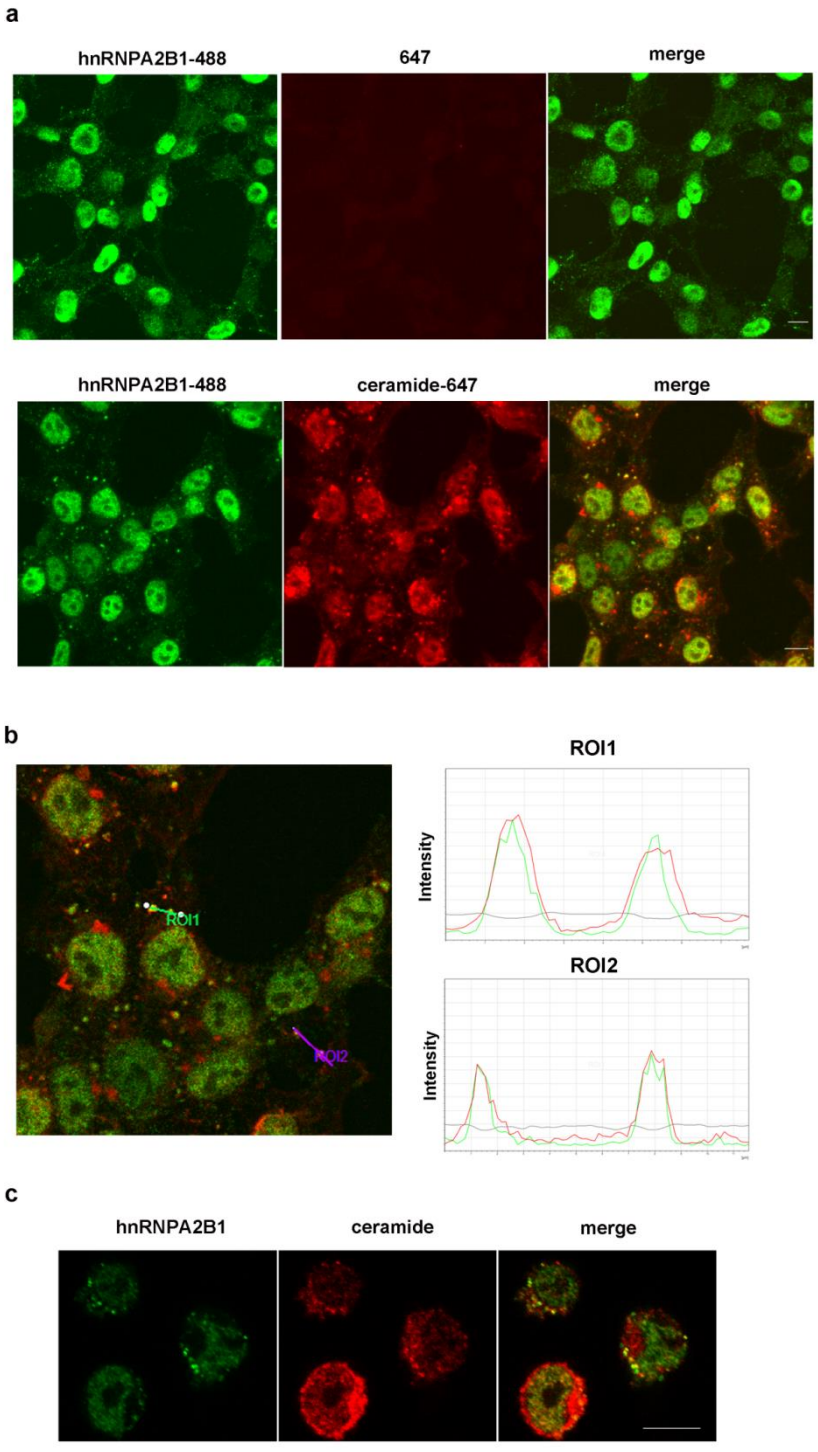

Supplementary Figure S5. HnRNPA2B1 presence in Multivesicular Bodies. (a) Confocal microscopy analysis of hnRNPA2B1 (green) and ceramide (red) co-localization in the cytoplasm of HEK293T cells. Negative controls without anti-ceramide primary antibody are also shown. Images show maximal projections of confocal images. Scale bar, 10 μm. **(b)** Confocal analysis of hnRNPA2B1 and ceramide co-localization. The images show one representative confocal section (magnification of the inset in (a)) and the intensity diagrams of the indicated regions of interest (ROI) **(c)** Confocal microscopy analysis of hnRNPA2B1 and ceramide co-localization in the cytoplasm of Jurkat T cells. Scale bar, 10 μm.

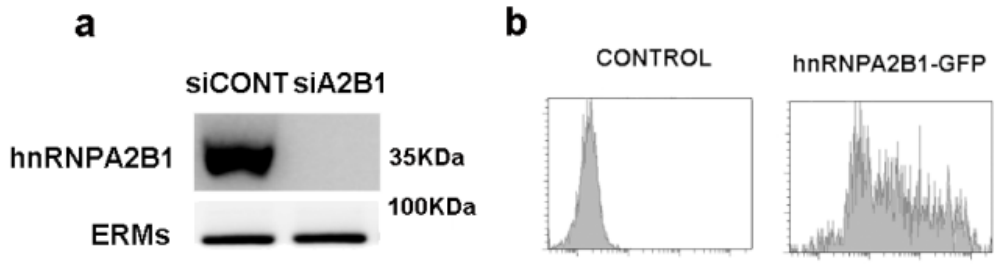

Supplementary Figure S6. (a) HnRNPA2B1 silencing and overexpression. (a) Representative western blot showing silencing of hnRNPA2B1 in cells transfected with specific siRNAs. **(b)** FACS analysis showing the overexpression of hnRNPA2B1-GFP.

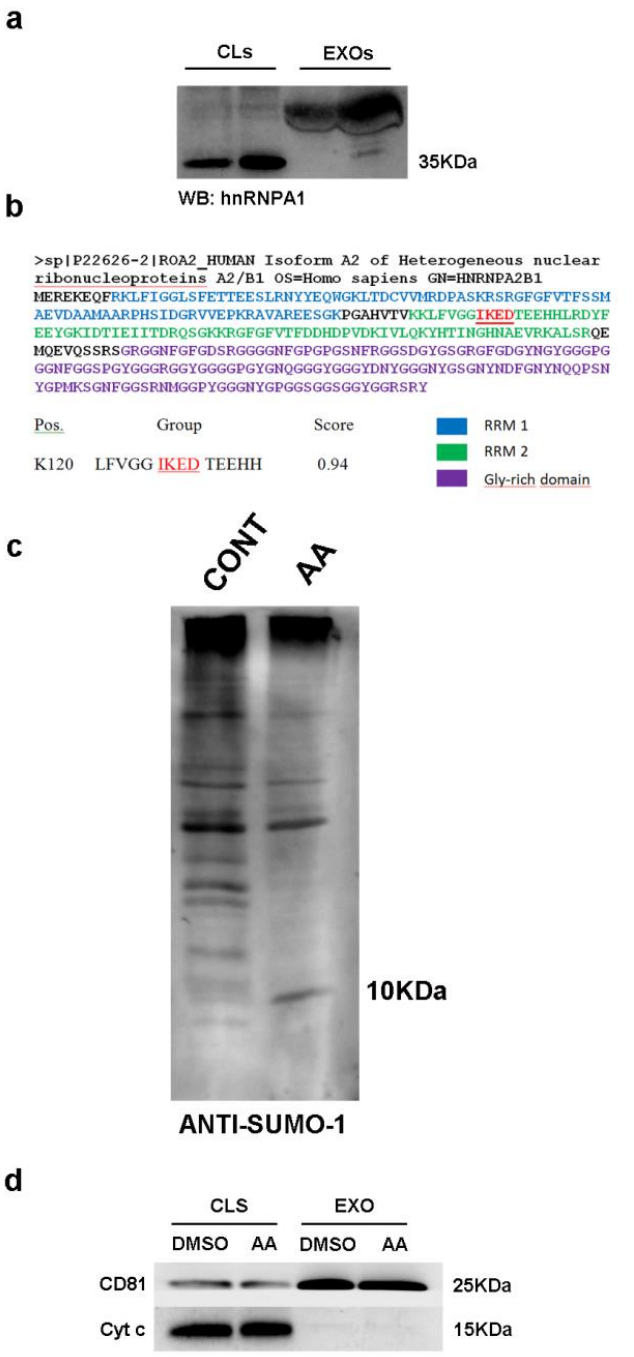

Supplementary Figure S7. Assessment of sumoylation inhibitor efficiency. (a) Western blot analysis of hnRNPA1 in T cells and their exosomes. **(b)** *In silico* analysis of hnRNPA2B1 putative sumoylation sites (Sumoplot) **(c)** Representative western blot showing the decrease in sumo-conjugated proteins in the presence of anacardic acid. Cells were incubated with anacardic acid (AA) or DMSO (control condition, CONT) and cell extracts were blotted for SUMO-1. **(b)** Representative western blot showing no changes in exosome secretion and cell death in the presence of anacardic acid. Cells were incubated with anacardic acid (AA) or DMSO (CONT), and exosomes were purified by ultracentrifugation and blotted for CD81 and cytochrome c.

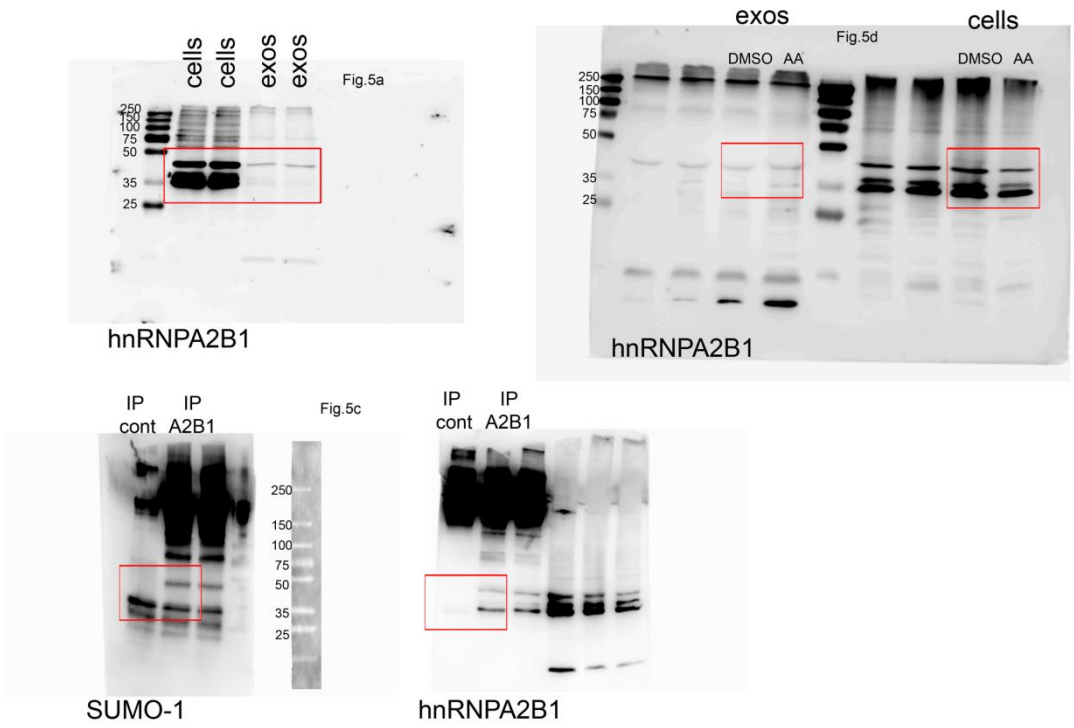

Supplementary Figure S8. Full immunoblots. Full immunoblots with indicated areas of selection as shown in Fig. 5.

Functions Annotation	p-Value	Molecules
processing of RNA	2,93E-10	"CDC42,DDX39A,DKC1,HNRNPA1,HNRNPA2B1,HNRNPU,HNRPDL, RBM39,RBM6,RPL14,RPL26,RPS16,RPS6,RPS7,SRSF2,SRSF3,SRSF5,TRA2A"
modification of rRNA	6,01E-06	DKC1,RPL14,RPL26,RPS16,RPS6,RPS7
annealing of RNA	7,88E-06	HNRNPA1,HNRNPC,HNRNPU
processing of rRNA	8,23E-05	RPL14,RPL26,RPS16,RPS6,RPS7
splicing of RNA	1,38E-03	CDC42,DDX39A,HNRNPA1,SRSF2,SRSF3,TRA2A
processing of mRNA	2,09E-03	DDX39A,HNRNPA1,HNRNPA2B1,SRSF2,SRSF5,TRA2A
splicing of mRNA	5,32E-03	DDX39A,HNRNPA1,SRSF2,TRA2A

Supplementary Table S1. miRNA-precipitated proteins related with RNA postranscriptional modifications. Ingenuity analysis identified "RNA posttranscriptional modifications" as the main cellular function related to miRNA-precipitated proteins (p-value 2.93E-10 – 5.32E-03).

SUPPLEMENTARY METHODS

Fluorescence confocal microscopy. For immunofluorescence assays, cells were plated onto slides, incubated for 12h, fixed and stained with the indicated primary antibodies (5 μg ml $^{-1}$) followed by alexa488- or alexa647-labeled secondary antibodies (5 μg ml $^{-1}$). Samples were analyzed with a Leica SP5 confocal microscope (Leica) fitted with a ×63 objective, and images were processed and assembled using Leica software. Fluorescence quantification was performed using ImageJ software. Co-localization analysis was performed with LAS AF software.

Subcellular fractionation. Jurkat T cells subcellular compartments were fractionated with Subcellular Proteome Extraction kit (Calbiochem). Cytosol, Membranous organelles and nucleus fractions were blotted for hnRNPA2B1, tubulin (cytosol marker), CD81 (membrane marker) and Histone 4 (nucleus marker)**.**

Buffer composition

Buffer 1: TBS pH7.5, 0.5% NP-40, 2.5mM $MgCl_2$, 40U ml^{-1}RNAse inhibitor (Invitrogen) and protease inhibitors (Complete, Roche)

Buffer 2: TBS, 0.05% NP-40, RNAse inhibitor and protease inhibitors

Buffer 3: PBS, 0.01% Tween

Buffer 4: 25mM Tris pH8, 150mM NaCl, 2mM $MgCl_2$, 0.5%NP-40, 5mM DTT, protease inhibitors and 40U/ml RNAse inhibitor (Invitrogen).

Buffer 5: 25mM Tris pH8, 900mM NaCl, 2mM $MgCl_2$, 1%NP-40, 5mM DTT, protease inhibitors and 40U/ml RNAse inhibitor.

Buffer 6: 25mM Tris pH8, 150mM NaCl, 2mM $MgCl_2$, 0.05%NP-40, 5mM DTT, protease inhibitors and 40U/ml RNAse inhibitor.

EMSA buffer: 10mM HEPES pH7.3, 5mM $MgCl_2$, 40mM KCl, 1mM DTT, 5% glycerol, 5μg tRNA.

Sequences of biotinylated miRNAs

miR-17: Bi.<u>CCCUCUUA</u>CAAAGUGCUUACAGUGCAGGUAG

miR-198: Bi.<u>CCCUCUUA</u>GGUCCAGAGGGGAGAUAGGUUC

miR-198mut: Bi.<u>CCCUCUUA</u>GGUCCAGAGUGCAGAUAGGUUC

miR-601: Bi. <u>CCCUCUUA</u>UGGUCUAGGAUUGUUGGAGGAG

Underlined nucleotides denote the 8-nt linker used to avoid direct binding of biotin to the miRNA (previously used in Heo *et al*.[49]).

SUPPLEMENTARY REFERENCES

49 Heo, I. *et al.* TUT4 in concert with Lin28 suppresses microRNA biogenesis through pre-microRNA uridylation. *Cell* **138**, 696-708 (2009).